ADVANCED MATERIALS INTERFACES
Open Access
www.advmatinterfaces.de

Lab-in-a-Bead: Magnetic Janus Bead Probe for the Detection of Biomarkers in Blood

Udara Bimendra Gunatilake, Adriana Caballe-Abalos, Sandra Garcia-Rey, Jon Mercader-Ruiz, Lourdes Basabe-Desmonts, and Fernando Benito-Lopez**

Remotely handled miniaturized colorimetric sensor platforms with multiple functionalities are able to mimic conventional laboratory operations with reduced assets. The integration of a magnetic phase in a miniaturized hydrogel sensor system allows the manipulation of the sensor, under a magnetic field, in a programmable manner. However, dark color interferences from conventional magnetic phases (Fe_3O_4, Fe_2O_3, and Fe micro/nanoparticles) affect the signal readout, hindering the colorimetric response. Therefore, a novel Janus bead configuration is introduced and tested by the localized incorporation of ferromagnetic iron microparticles into a TiO_2 nanotubes/alginate hydrogel bead biosystem, under an applied magnetic field. The so-called hydrogel Janus bead shows both, magnetic translocation and biosensing properties in the same bead. These beads are used for the direct colorimetric analysis of biomarkers in blood. The surface of the Janus bead prevents the biofouling of red blood cells, keeping the sensor surface clean for accurate optical colorimetric analysis. Moreover, the external magnetic manipulation of the bead permits precise control of the time and position of the bead in the sample. Therefore, multiple functionalities are presented by a single magnetic TiO_2 nanotubes/alginate Janus bead such as actuation, low biofouling, and sensing, positioning this technology as a truly Lab-in-a-Bead System.

1. Introduction

Colorimetric signal reading is becoming a very promising detection technology for portable and Point of Care (POC) devices due to its power-free, simple operability, portability, and low-cost.[1–3] In particular, solid or semi-solid materials with immobilized colorimetric assays integrated in miniaturized colorimetric sensors continue appearing in the literature, where hydrogels are rising as promising materials.[4,5] They provide a water-rich solid matrix capable of loading and immobilizing the required colorimetric assay to perform the desired detection.[4] For instance, glucose oxidase (GOX) and horseradish peroxidase (HRP) were used as enzymatic catalysts, and 3,3′,5,5′ tetramethyl-benzidine (TMB) as a chromophore for the detection of glucose.[6] Therefore, a safe and stable immobilization of the enzymes and chromophores on the solid platform plays an important role in accurate sensing. However, fast drying is a drawback in hydrogel-based sensors, since the absorbed water into the polymer network easily evaporates under environmental conditions. This is usually addressed by storing the hydrogel in a sealed container or by keeping it in a moist environment. Moreover, the molecules of the assay, entrapped in the hydrogel sensing scaffold, usually diffuse to the surrounding analyte solution over time since they are immobilized through weakly bound physical bonds. This causes ionic densities to be imbalanced between

U. B. Gunatilake, A. Caballe-Abalos, S. Garcia-Rey, J. Mercader-Ruiz, F. Benito-Lopez
Microfluidics Cluster UPV/EHU
Analytical Microsystems & Materials for Lab-on-a-Chip (AMMa-LOAC)
Group Analytical Chemistry Department
University of the Basque Country UPV/EHU
Leioa 48940, Spain
E-mail: fernando.benito@ehu.eus

The ORCID identification number(s) for the author(s) of this article can be found under https://doi.org/10.1002/admi.202202459

DOI: 10.1002/admi.202202459

U. B. Gunatilake, A. Caballe-Abalos, S. Garcia-Rey, J. Mercader-Ruiz, L. Basabe-Desmonts
Microfluidics Cluster UPV/EHU, BIOMICs Microfluidics Group
Lascaray Research Center
University of the Basque Country UPV/EHU
Vitoria-Gasteiz 01006, Spain
E-mail: lourdes.basabe@ehu.eus

J. Mercader-Ruiz
Arthroscopic Surgery Unit
Unidad de Cirugía Artroscópica (UCA)
Vitoria-Gasteiz 01008, Spain

L. Basabe-Desmonts
Basque Foundation of Science
IKERBASQUE
Bilbao 48013, Spain

the hydrogel and the outer solution, leading to a reduction in the amount of reactants needed for detection inside the hydrogel scaffold over time.[7] In this regard, as a problem-solving technique, the fast removal of the scaffold from the solution, using a smart remote-controlled manipulation system, could reduce or eliminate assay leaking from the hydrogel scaffold.

Biocompatible and remotely manipulable organic-inorganic hybrid materials offer tremendous applicability when integrated into biosystems.[8,9] In particular, magneto-driven actuators provide a good alternative when compared to other types of remote stimuli, such as temperature, electricity, or light.[10] Zhao et al. presented a lab-in-a-droplet system based on superhydrophobic magnetic particles able to encapsulate reagents and samples. The interior of the droplet was addressable by applying the magneto-induced shell opening and closing properties of the magnetic liquid marbles.[11] Nevertheless, the integration of the magnetic phase in hydrogel-based miniaturized sensor scaffolds is required to ensure their manipulation. In this regard, in situ or ex situ nano/micro structured magnetic inorganic phases can be incorporated into the hydrogel matrix not only to promote remote controllable responses but also to increase the mechanical properties of the hydrogel.[12,13] The incorporation of magnetic properties into the sensor scaffold facilitates the remote manipulation of the scaffold, even in a programmable manner, and it could bring new applicability to the microfluidic sector. Moreover, this remote manipulation can be used to minimize the leaching of the assay by promoting the fast separation of the scaffold from the analyte solution, using an external magnetic field. However, the intrinsic dark color of most commonly used magnetic particles (e.g., Fe_3O_4 –black, γ-Fe_2O_3 –brown, Fe –grey) interferes with the colorimetric system, by distracting the optical signal reading. Therefore, the fabrication of magneto-driven hydrogel colorimetric systems is challenging when using conventional magnetic materials.

In addition to that, the colorimetric analysis of biomarkers in whole blood, which is the gold standard biofluid used for health care, persists as a complicated and costly operation due to the interference of the red color from the hemoglobin with the optical read-out system.[14] In this regard, before analysis, whole blood needs to be separated into plasma or serum prior to biomarker detection. On laboratory premises, systems that use mechanical forces, such as centrifuges, are commonly used to separate red blood cells from plasma. Moreover, when using miniaturized systems or point-of-care devices, although sedimentation and external field-based systems like acoustic, electrical, and magnetic are also used,[15] nonetheless filter membranes[16,17] are more widely employed. However, the challenge faced by this type of analysis is to avoid the red blood cells (RBC) separation additional step, which leads to complicated and costly instrumentation or to the fabrication of sophisticated detection systems for whole blood detection. Park et al.[18] reported a 3D printed plasma separating membrane where RBCs were filtered out and plasma was moved to the detection zone to analyze glucose from whole blood. Recently, Xu et. al.[19] introduced a hydrogel/paper-based analytical device, and Jing et. al.[20] developed a nanometer scale porous structured poly(ethylene) glycol-diacrylate hydrogel disc with an immobilized glucose sensing assay for the direct colorimetric measurement of glucose in whole blood. In this system, the glucose diffuses through the hydrogel matrix while preventing RBCs from interfering with the sensing signal in a single-step blood analysis protocol. Divergently, Russel et. al.[21] introduced self-propelled Janus particles, which were able to detect particle motion change colorimetrically. In this case, bimolecular interactions triggered changes in the particle´s (colored iron oxide core) motion that were detected as variations in color when spotted on paper. The system was used to detect a sepsis biomarker in whole blood.

In previous scientific records, microfluidic synthesis protocols were mostly used to synthesize magnetic Janus beads. Yin et al.[22] fabricated magnetic-fluorescent responsive Janus supraballs in a microfluidic device with a two-needle microchannel, forcing two separate oil solutions to simultaneously flow. Dichloromethane/QD (quantum dots) polymer hybrid and dichloromethane/ionomers/Fe_3O_4 nanoparticles flowed separately through the needles, and the separate drops merged into a large one at the exit tip by the surrounding water stream, achieving Janus supraballs with distinct hemispherical regions after dichloromethane evaporation. In addition, Kang et al.[23] fabricated Janus microbeads having sensory polydiacetylenes (PDA) liposomes and magnetic nanoparticles by sending the two solutions of alginate/PDA liposome and alginate/magnetic particles separately from two needles and coupling together at the end of the tip, allowing to form a single drop, followed by cross-linking with calcium ion bath. The possibility of introducing magnetic field-aided Janus bead fabrication protocols provides a simple process that avoids utilizing complicated tools or processes.

Herein, a novel magneto-driven hydrogel Janus bead with multiple functionalities is presented as a Lab-in-a-Bead system. Magnetic properties were integrated into the TiO_2 nanotubes (TNT)/alginate hydrogel optical biosensor bead by introducing superhydrophobic Fe particles to the polymer matrix, in which the polymer nanocomposite was cross-linked under a specific magnetic field-induced protocol. The synthesized Janus bead showed efficient optical biosensing (glucose was tested as a model) and, at the same time, magneto actuation properties. Moreover, the Janus bead acted as a membrane to repel the red blood cells from the blood, minimizing red color artifacts during colorimetric sensing. This Lab-in-a-bead system opens new avenues for the magneto-programmable, colorimetric detection of blood biomarkers in a simple and cheap manner, acting as a probe when immersed in blood.

2. Results and Discussion

2.1. Synthesis and Characterization of the Janus Bead

The integration of magnetic particles into a hydrogel bead darkens its coloration, restricting the possible applicability of the bead for colorimetric signal analysis. In order to avoid the interference of the dark coloration of the bead, the magnetic hydrogel bead was synthesized following the protocol presented in the Experimental Section (fabrication of the Janus bead), combining both properties, the colorimetric sensing and the magneto-driven capability in the same matrix, called Janus bead. As demonstrated in **Figure 1**a, a droplet of TNT/ C_8-Fe/alginate polymer blend was dripped onto the cross-linking Ca^{2+} solution under a 353 mT vertical gradient magnetic field. The COO^- groups of the alginate in the polymer blend droplet, started to cross-link with the Ca^{2+} cations over all the interface of the droplet with the calcium ions

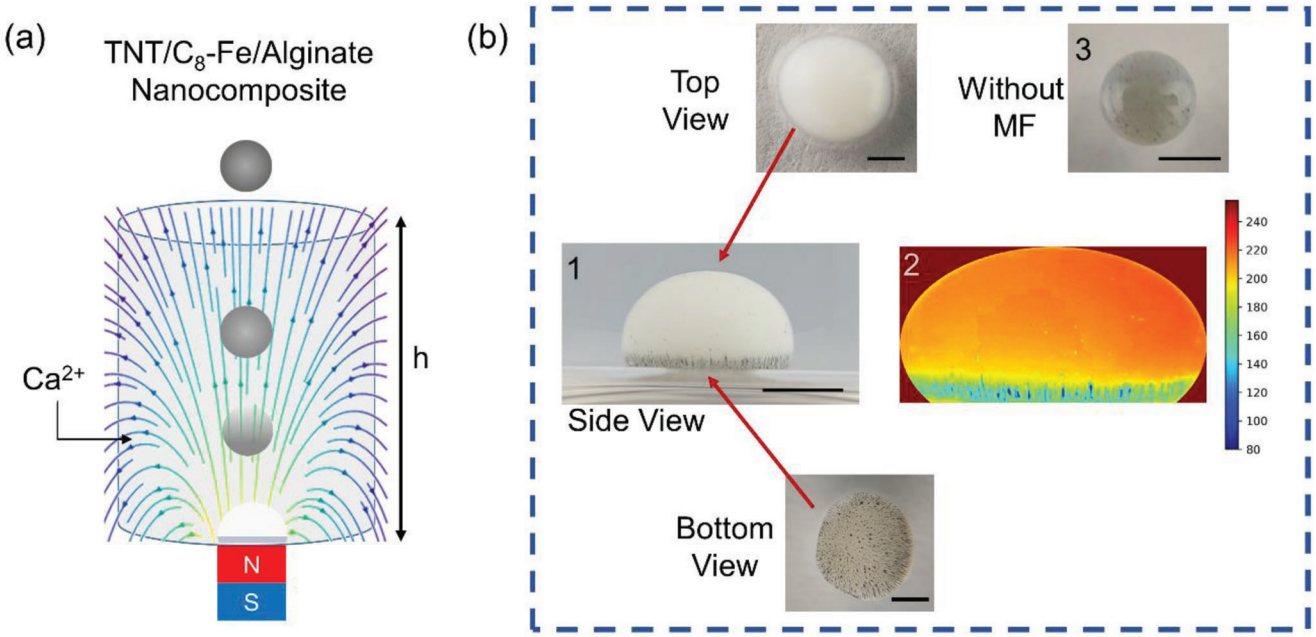

Figure 1. a) Schematic illustration of the fabrication of a Janus bead under an applied gradient magnetic field, (magnetic flux density indicated with lines). b) Side, top, and bottom views of the fabricated Janus bead (set of picture 1). Illustration of the absence of interference from the magnetic particles in the sensing readout area by a color map (picture 2). TNT/C_8-Fe/Alginate bead fabricated without a magnetic field (picture 3). Scale bars indicate 2 mm length.

solution, immediately after the droplet touched the solution.[24] At the same time, the magnetic particles present in the polymer blend were attracted to the magnet, following the magnetic field lines as shown in Figure 1a. However, the instantly cross-linked flexible TNT/alginate polymer shell of the bead prevents the physical separation of the magnetic particles from the polymer blend. Therefore, the magnetic phase got deposited at the bottom of the bead, forming a hemispherical magnetic bead (≈4.3 mm), as shown in Figure 1b (picture 1). The force applied to the soft polymer by the magnetic particles led to the flattening of the bottom of the bead, whereas a spherical shape was observed when the magnetic field was not applied.

However, partial contamination of the sensing area with residual magnetic particles was observed during the fabrication process. The 3D network of the polymer (TNT/alginate), which formed rapidly, prevented the movement of the magnetic particles to the bottom of the bead, contaminating the top part of the bead. In order to minimize this process, the Fe particles were chemically modified with alkyl chains (superhydrophobic C_8-Fe particles) to avoid interactions with the superhydrophilic TNT/alginate suspension. Moreover, the concentration of the Ca^{2+} cross-linker in the solution was reduced to 0.2 M (from the usual concentration of 0.4 M used for the fabrication of non-magnetic alginate beads[4]) to avoid the rapid cross-linking of the polymer shell. This allowed the magnetic particles to reach the bottom of the bead, minimizing their trapping, during cross-linking, in the sensing region of the bead. In addition, the height (h) of the cross-linking bath was investigated. The induction of the magnetic field on the hydrogel bead is reduced while increasing the value of h thus, for h > 10 mm, the upper surface of the bead is contaminated with magnetic particles. Therefore, h was set to 10 mm in order to be able to apply high magnetic forces to the system and rapidly confine the magnetic particles at the bottom of the bead. During the Janus bead fabrication process, the magnetic particles move to the depth of the bead due to the applied gradient field while the alginate polymer cross-links by the Ca^{2+} ions. The assay droplet including magnetic particles rapidly cross-linked with the Ca^{2+} ions and formed an external outer layer of alginate as a capsule according to the egg-box model. Then, the Ca^{2+} cations penetrated through the capsule to fully cross-link the alginate polymer to form the 3D bead.[12,25] The magnetic particles are physically trapped within the hydrogel at the bottom of the bead heterogeneously. No leaching of particles was observed during or after the process. Figure 1b, clearly shows a picture of a bead with no color interference from the magnetic particles, when using this optimized protocol, facilitating the monitoring of possible optical signals coming from the white surface of the bead. A magnetic bead, fabricated without the magnetic field is shown in Figure 1b (picture 3), where it is easy to observe the difference in color. The color map of the Janus bead, side view in Figure 1b (picture 2), clearly illustrates the separation of the magnetic phase (blue/green) and the TNT/alginate sensor phase (orange). Moreover, B&W value histograms (see Figure S1, Supporting information) demonstrated that the average of the B&W value increased to 206 from 118 in beads where the magnetic field was applied during their fabrication process. In addition, Energy Dispersive X-ray (EDX) analysis of the top and bottom areas of the beads indicated a significantly low Fe percentage in the upper surface when compared to the bottom area (Tables S1 and S2, Supporting Information). It is possible to observe that the magnetic particles are self-assembled vertically, following the magnetic flux lines at the bottom of the bead

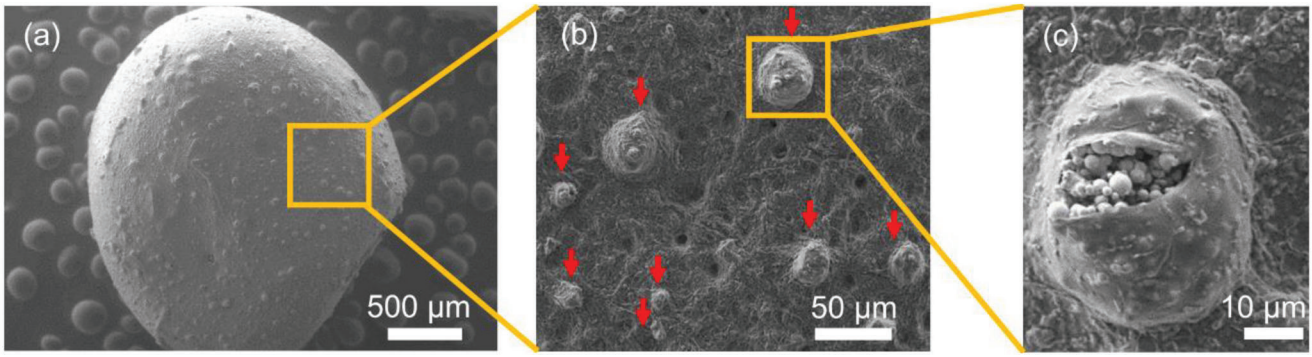

Figure 2. SEM images (cryo mode) of the bottom side of the Janus bead, a–c) increasing the magnification while focusing on the magnetic particles accumulated spots ↓.

(Figure 1b-1), which provide the magnetic properties to the Janus beads.

The efficiency of the fabrication of the Janus bead depends on the magnetization of the particles and the applied magnetic field. However, conventional superparamagnetic iron oxide (magnetite or maghemite) nanoparticles (5–20 nm) show low magnetization[26] and thus, the current applied magnetic field is not sufficient to rapidly attract the magnetic particles to the depth of the bead, leading to contamination of upper surface or the sensing area with particles. Therefore, iron microparticles (1–10 µm), which show sufficient magnetization (approximately three times higher saturated magnetization), were used for a rapid attraction of the particles towards the depth of the bead while cross-linking, avoiding contamination of the upper surface or the sensing area.

The surface morphology of the Janus bead was investigated, **Figure 2**. A bumpy surface on the bottom side of the bead was obtained due to the embodiment of the magnetic particles, as shown in Figure 2a. The magnetic particles were attracted to the bottom side, following the magnetic flux lines of the magnet. Therefore, these particles covered the hydrogel and formed bumpy spots (red arrows in Figure 2b) on the surface. A cracked polymer layer in a bumpy spot is shown in Figure 2c where the magnetic particles were clearly seen inside the polymer. Moreover, the non-binding behavior of each individual particle to the polymer was clearly visible. The perfectly spherical shape of the particles is visible and reminds separate from the polymer matrix, due to the superhydrophobicity of the C_8-Fe particles. In Figure 2c, the edge or the corner of the sample has fractured due to the rapid freezing in the cryo-SEM morphology analysis process, not in the fabrication process. Cracking or damage to the beads, after fabrication or gentle manipulation, was not observed. Since the Janus bead operates in its hydrated state, beads resist mild friction or shock due to the elasticity of the hydrogel in its hydrated state. In the worst scenario, if the hydrogel cracks and the bead lose some of the magnetic particles due to high friction, the particles could accumulate over the magnet, diminishing the overall manipulation efficiency of the bead rather than its sensing efficiency.

The dehydration of the hydrogel could reduce the sensing performance since the activity of the enzymes could get reduced, while the absorption of analytes is not very efficient in the dried state. To avoid this, the scaffolds were stored in a moistened, sealed, and low temperature (5–25 °C) condition to keep the enzymes and the assays in an active domain. The sensing performance was stable without presenting any significant performance issues, even after 10 days of storage.

2.2. Remote Stimuli Janus Bead

The magnetic properties of the freeze-dried Janus beads were characterized by SQUID superconducting quantum interference device (SQUID) and vibrating-sample magnetometer (VSM) magnetometers, **Figure 3**a. The octyl-alkyl chain coating on the ferromagnetic Fe particles reduced the saturation magnetization of the particles to 220 from 239 $Am^2\ kg^{-1}$ due to the addition of the non-magnetic octyl-alkyl to the magnetic particles. Particles can bridge together and get functionalized with the carbon chains during the synthesis protocol. Figure S2a,b (Supporting Information) shows the non-aggregated and aggregated particles. The size and morphology of the particles were analyzed in our previous paper.[27] These aggregations lead to magnetic dipole–dipole interactions and/or exchange interactions, which are couplings of the magnetic moments in neighboring atoms, significantly affecting the magnetic properties of the particles, showing a significant hysteresis in the magnetic curve loop.

A saturation magnetization of 49 $Am^2\ kg^{-1}$ was expected when adding 22.3% (w:w) of C_8-Fe to the pre-hydrogel nanocomposite prior to the synthesis of the Janus bead, according to the weight ratios of magnetic components (220 $Am^2\ kg^{-1} \times 0.223$) in the composite, but the obtained value was just 22 $Am^2\ kg^{-1}$. The 20 µL of the composite suspension that used to cross-link the bead in the Ca^{2+} solution does not represent the same magnetic particle concentration as calculated, due to the non-homogeneous distribution of the low surface energy C_8-Fe particles in the pre-gel solution (non-favorable hydrophobic and hydrophilic attractions), see Pictures of the distribution of the magnetic particles in Figure 1 and in the SEM images in Figure 2 for the final bead. Moreover, the non-magnetic calcium cross-linkers could also lead to a reduction (in this case) the magnetization of the bead, lowering the saturation value. Concerning the magnetic characterization, it can be concluded that 10% of C_8-Fe is present in the Janus bead by considering that the magnetic properties remained the same during the hydrogel synthesis and the freeze-dried protocols.

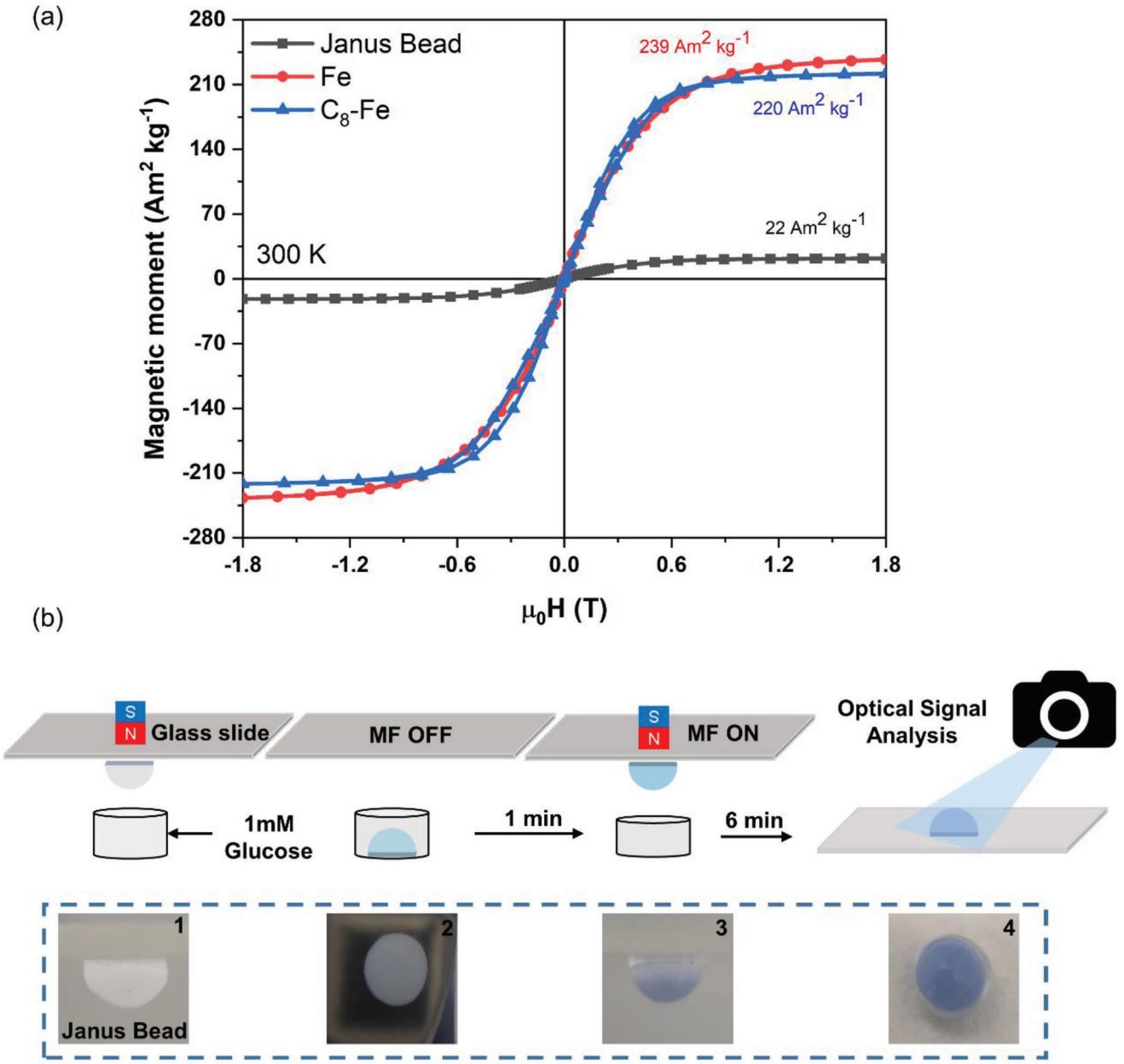

Figure 3. a) Magnetization (M–H) loops of the Fe, C_8-Fe, and Janus bead (freeze-dried), which were recorded by SQUID and VSM at room temperature. b) Scheme of the magneto manipulation of the Janus bead. The bead was dripped into a 1 mM glucose solution and removed after 1 min using magnetic attraction. Real images of the Janus bead for each step of the process are depicted behind each of the steps.

Remote manipulation of hydrogel sensor scaffolds facilitates the building of programmable devices and addresses the inherent problems faced by hydrogel-based sensors. For instance, the diffusion of the sensing assay, presented inside the hydrogel, out of the solution is a major problem in hydrogel-based sensors.[7] Figure S3 (Supporting information) shows the diffusion of the encapsulated reactants in a conventional alginate hydrogel to the analyte solution, where the reaction is taking place outside the hydrogel sensor. This leaching process can be minimized by just separating the hydrogel bead from the bulk solution in a controlled manner and over a controlled period of time. Moreover, the manipulation of the beads in a device can be difficult and could require extra components, which might diminish the functionality of the final device and its possible miniaturization. In this case, the magnetic property of the Janus bead can be used to manipulate and control the bead's position remotely, and to manage the time the bead is in contact with the solution to be analyzed. Figure 3b shows the controllability of the Janus bead by just using a 1 × 1 cm NdFeB magnet. First, the Janus bead was dripped into a 1 mM glucose solution and collected back after 1 min. This process reduced the possible leakage of the colorimetric assay reagents, present in the bead, due to diffusion. Once

out of the solution, the bead was left to react with the glucose soaked into it and the colorimetric signal was recorded at 6 min. This process was also investigated using a simple microfluidic device configuration. Remote handling and transportation, using a magnet, of the Janus bead inside a microfluidic channel, while glucose is detected, is shown in Video S1 (Supporting Information).

2.3. Non-Interference of the Red Blood Cells into the Janus Bead

Blood consists of ≈45% of red blood cells (RBCs), <1% of white blood cells and platelets and 54% of plasma. Plasma is mainly water with dissolved proteins and other biomolecules such as glucose, lactic acid, uric acid, cholesterol, and salts.[17] The fabrication of a one-step colorimetric detection of biomarkers in the blood remains challenging due to the hindering of the optical signal by the red coloration coming from the red blood cells. However, the use of the Janus bead was subjected to detect one of the most demanding biomarkers present in the blood, glucose.

The schematic illustration in **Figure 4**a shows the behavior of the Janus bead when immersed in blood. It was observed that the red coloration of blood, due to the RBCs, was not transferred to the Janus bead, even after remaining for 6 min inside the 1 mL blood container, as depicted in Figure 4b. This demonstrated that RBCs are too big to diffuse inside the bead due to the small mesh size (absence of micro range mesh) of the surface of the bead. In addition, the RBCs were filtered out from the outer surface of the Janus bead when removed from the solution. The cross-section of the Janus bead is shown in Figure 4c, where a high porosity (≈150 µm), considering the space between separated polymer petals, was observed. However, the outer surface of the Janus bead was formed by a ≈40 µm thick polymer layer, as shown in the Figure S4 (Supporting Information). SEM images of the outer surface of a hydrated and dehydrated Janus bead are shown in Figure 4d,e, respectively. They clearly showed a rough surface with absence of micro-pores or micron mesh size in the outer surface. Therefore, the surface of the Janus bead is able to block the entrance of the RBCs, which have a biconcave shape with a diameter of ≈8 µm and a thickness of ≈2.5 µm,[28] inside the bead. As well, the dimensions of the RBCs are much bigger than the reported mesh size of alginate hydrogels, 6–14 nm,[29] thus it is not possible for them to diffuse inside the Janus bead.

However, the hemolysis of RBCs in blood, which occurred due to osmosis while diluting blood samples, released the red-colored hemoglobin molecule (5 nm)[30] and entered the Janus bead, Figure 4f. In this case, a smart handling of the blood samples could avoid the red coloration of the Janus bead. For instance, the dilution of whole blood with PBS buffer avoids hemolysis and hemoglobin diffusion, as shown in Figure 4f (right side image).

The optical signal readout performance of the Janus bead was compared with that of a conventional sensing paper substrate. Figure 4g shows the glucose sensing assay absorbed into a paper substrate and into a Janus bead, using the same glucose assay ratio, as mentioned in the Experimental Section (Fabrication of the Janus Bead). Both scaffolds were subjected to the blood glucose detection protocol as mentioned in Experimental Section (Colorimetric Signal Readout Analysis) to check the signal readout. A clear blue color optical signal, due to glucose, was observed in the Janus bead since the RBCs got filtered out of the surface of the bead. This indicates the capability of the Janus bead to perform one single step glucose sensing in blood. On the other hand, the blue color optical signal was hindered on the conventional paper substrate due to the presence of red coloration coming from the RBCs, which got adhered to the surface of the paper.

2.4. Glucose Sensing by the Janus Bead

The Janus bead provides a versatile platform for enzymatic chemical reactions by keeping the reactants in a miniaturized scaffold with multiple functionalities, as explained above. **Figure 5**a top image shows a schematic diagram of the process occurring in the bead.[31] In brief, glucose was oxidized to gluconic acid while the oxygen was reduced to hydrogen peroxide in the presence of the glucose oxidase, an enzymatic catalyst, once the glucose molecules entered the bead. Then, the generated hydrogen peroxide was reduced to water by the enzymatic catalyst, horseradish peroxide, and the chromophore, TMB, was oxidized, generating a blue color in the bead. The intensity of the formed color relates to the concentration of the glucose, as shown in the Figure 5b bottom images, where different concentrations of glucose in blood were detected using the Janus bead. As recently demonstrated by us,[4] TiO_2 nanotubes in the hydrogel scaffold increased the sensing rate of the glucose, increasing the glucose absorption efficiency into the Janus bead due to their superhydrophilicity. The color signal was recorded at 6 min for the Janus bead, while 13 min was necessary for the bare alginate bead, without TiO_2 nanotubes, in order to obtain the same glucose concentration values.

The glucose detection performance by the Janus bead was evaluated in human blood, human plasma, and PBS solution. The B&W value difference of the Janus beads, before and after glucose detection, was analyzed from the captured images of beads at 0 and 6 min for five glucose concentrations. An increased color intensity (B&W difference) was observed when increasing the concentration of glucose in the different matrixes. Then, the calibration curves were generated. PBS, human plasma, and human blood calibration curves are depicted in Figure 5b–d, respectively. Linear dynamic ranges, at 6 min recording time, were obtained for the three samples within a glucose range of 0.1–0.8 mM, showing highly reliable correlation coefficients, $R2 > 0.99$, from the linear regression analysis. The statistical limit of detection (LOD) was calculated to be 0.05 mM with a limit of quantification (LOQ) of 0.16 mM for glucose in PBS solution ($LOD = 3S\ K^{-1}$, and $LOQ = 10S\ K^{-1}$, where S is the standard deviation of the blank sample and K is the slope of the calibration curve). However, the evaluation of the LOD and LOQ was not possible in the case of blood and plasma due to the difficulty in obtaining a zero concentration glucose blank value, as blood/plasma always contains glucose. However, a high deviation from the LOD/LOQ values in PBS should not be expected for blood/plasma detection by the introduced Janus bead.

A random blood sample (10 times diluted with PBS) was tested with the Janus bead to check the accuracy of the glucose concentration obtained by PBS, plasma, and glucose calibration curves, compared to a commercial glucometer. The obtained glucose

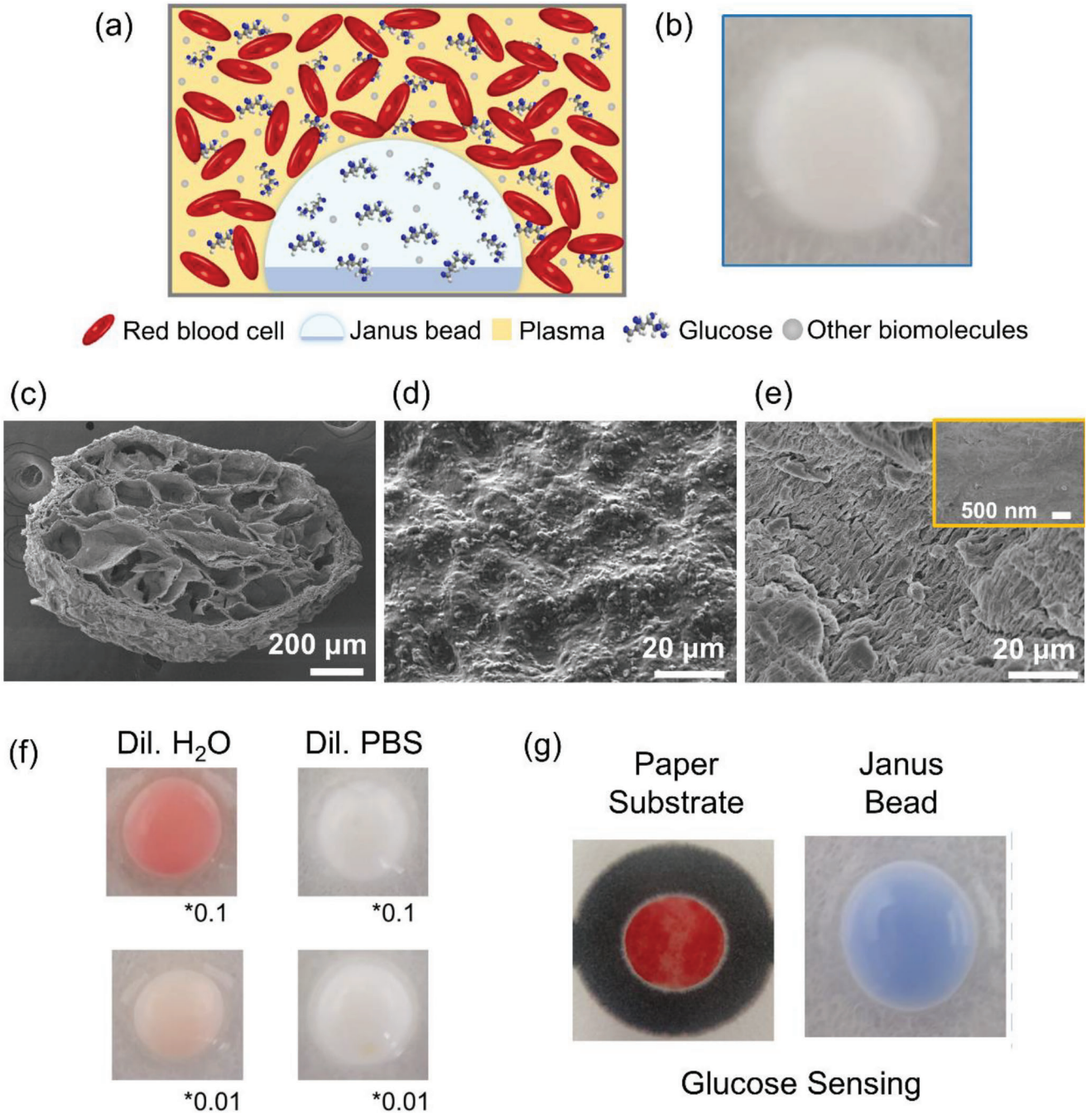

Figure 4. a) Schematic illustration of the diffusion of small molecules, like glucose, into the Janus bead avoiding the absorption of RBCs. b) The Janus bead (without sensing assay) after 6 min immersed in blood, 1 mL whole blood. The bead was rinsed with PBS before capturing the image, and the bead was magnetically handled throughout the process. c) SEM image of the cross-section of a freeze-dried Janus bead. d) Cryo-mode SEM image of the hydrated and swelled Janus bead surface and e) SEM image of the freeze-dried Janus bead surface, inset, represents a high magnification image of the surface. f) Janus bead (without sensing assays) after 6 min. remain inside the 1 mL diluted blood with water and PBS under (*0.1) 10 and (*0.01) 100 dilution factors. g) Glucose detection using a sensing assay loaded in a conventional paper substrate and in a Janus bead.

concentrations from the Janus bead analysis (**Table 1**) for the plasma and the blood calibration curves showed nearly the same values as the ones obtained with the instant commercial glucometer. On the other hand, the glucose concentration obtained for the PBS solution significantly deviated from the glucometer values. This unexpected result could be explained by considering the artificial PBS sample, which is not an ideal matrix for the quantification of glucose using the commercially available glucometer as opposed to the real blood and plasma sample matrixes. Nevertheless, the results obtained when using the Janus

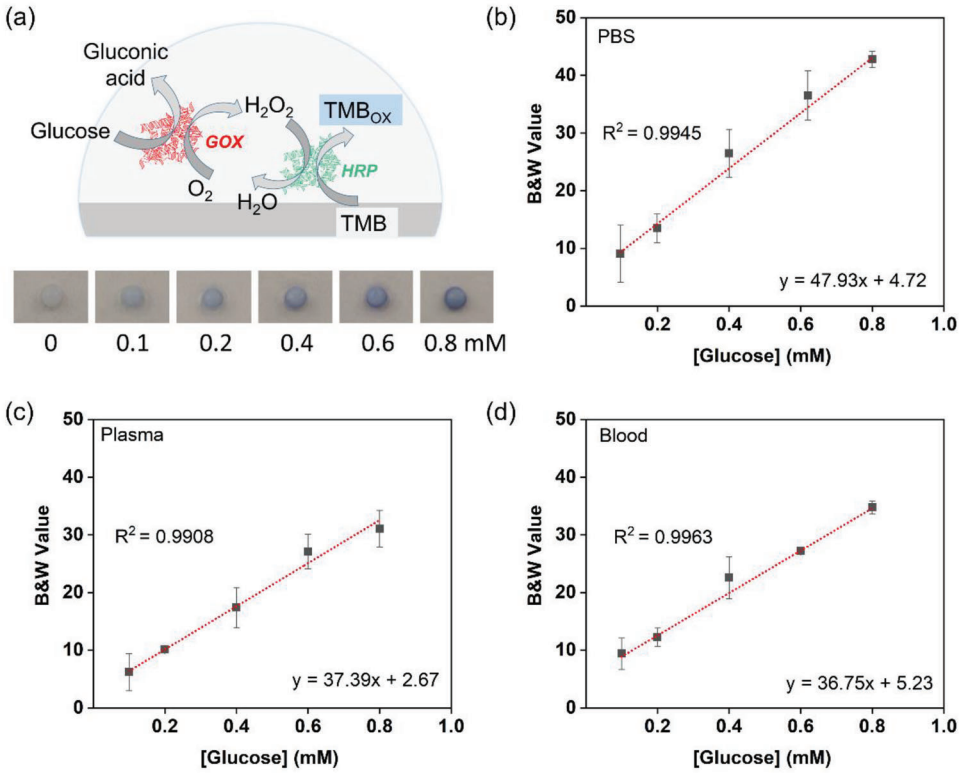

Figure 5. a) Schematic diagram of glucose detection in the Janus bead (top side) and pictures of the Janus beads (bottom side) at different glucose concentrations in blood, taken at 6 min time. Calibration curves for glucose in b) PBS solution, c) human plasma, and added glucose in d) human blood by using the Janus bead. Error bars correspond to mean values ± SD ($n = 3$).

beads present a promising multifunctional applied material for the colorimetric determination of glucose concentrations in complex samples such as blood.

3. Conclusion

We introduce the Lab-in-a-Bead concept by fabricating a novel Janus bead with magneto-driven and colorimetric sensing capabilities. The introduction of low surface energy ferromagnetic Fe microparticles into the TNT/alginate hydrogel and the subsequent cross-linking under a controlled magnetic field, facilitate the fabrication of a novel sensing Janus bead with actuation capabilities. The fabrication avoids the conventional dark color interference into the bead due to the magnetic phase.

The Janus bead provides a versatile platform to immobilize assays for colorimetric sensing, due to its moisture conditions and the white background color of the bead. Moreover, the configuration of the Janus bead is able to filter out the RBCs from whole blood samples and colorimetrically detect the desired biomarkers, e.g. glucose, without the need to apply RBCs removing protocols like centrifugation or the use of filters. Therefore, the multiple functionalities of this novel Janus bead such as remote handling, magnetic manipulation, assay reagent immobilization and storage, RBC filtration, and biosensing demonstrate the concept of Lab-in-a-Bead.

Table 1. Comparison of blood glucose concentrations in the sample obtained using the glucometer and the Janus beads by the different calibration curves, ($n = 3$).

Glucometer	Calibration curves		
	PBS	Plasma	Blood
5.0 ± 0.2 mM	3.5 ± 0.3 mM	5.0 ± 0.9 mM	4.4 ± 0.2 mM

4. Experimental Section

Synthesis of TiO_2 Nanotubes: First, TiO_2 nanoparticles were synthesized by a precipitation method similar to the one described in the reference.[32] Briefly, a titanium precursor solution was prepared by adding 5 mL of titanium isopropoxide (97%, Sigma–Aldrich, Spain) to 15 mL of isopropanol (EssentQ, Sharlab, Spain). The solution was transferred to a 250 mL distilled water (pH ≈2 by 1 M nitric acid (65%, Sigma–Aldrich, Spain) solution, under vigorous stirring. Hydrolysis of titanium isopropoxide occurred rapidly, showing a turbid solution. Then, the solution was heated at 60 °C under stirring for 12 h. Then, the precipitate was washed with water and ethanol three times and the particles were separated by rotary evaporation at 60 °C, under vacuum.

TiO_2 nanotubes were synthesized by a hydrothermal method using the synthesized TiO_2 nanoparticles.[33] TiO_2 nanoparticles (1.0 g) were stirred in 20 mL of 10 M NaOH (98%, Sigma–Aldrich, Spain) for 2 h. Then, the basic titania dispersion was transferred to a Teflon-lined hydrothermal autoclave vessel and was heated at 150 °C for 48 h inside the furnace. The

precipitate was removed after the vessel was cooled to room temperature and was washed with water and 0.1 M HCl (37%, Sigma–Aldrich, Spain) until the pH of the synthesized TiO_2 nanotubes reached pH 7–8. Finally, the TiO_2 nanotubes were separated by rotary evaporation at 60 °C under vacuum.[4]

Synthesis of C_8-Fe Particles: Iron micro particles (1.00 g) (<10 micron, 99.5%, Alfa Aesar, Germany) were mechanically stirred in 5.0 mL of 0.25 M HCl for 15 min. Next, the particles were magnetically separated from the solution and washed with water, ethanol, and acetone respectively. Then the particles were dried for 1 h at 60 °C. Then, 1.8 mL of triethoxy(octyl)silane (97%, Sigma–Aldrich, Spain) was mixed with 50 mL of absolute ethanol (Sharlau, Spain) for 2 h at 50 °C. Later, a sonicated suspension of pre-treated 0.53 g of Fe particles in 10 mL absolute ethanol was added to the triethoxy(octyl)silane/ethanol solution and stirred for 2 h. After that, the particles were separated with a magnet and thoroughly washed with ethanol for three times. Finally, the particles were heated at 120 °C for 2 h to obtain C_8-Fe magnetic particles.

Fabrication of the Janus Bead: First, 5 mg of TiO_2 nanotubes were mixed with 1 mL of 1% (w/v) of alginate (Sigma–Aldrich, Spain) (1.00 g alginate/100 mL distilled water) for 15 min under sonication, followed by 48 h magnetic stirring (TNT/alginate polymer suspension). Next, 5 mg of C_8-Fe magnetic particles were added to the TNT/alginate composite and the mixture was vortexed for 5 min. Here, the hydrophobic C_8-Fe particles could not form a stable suspension with the TNT/alginate composite due to their unlikely attractions. Therefore, a high mechanical force was applied to load the C_8-Fe particles temporally (short time) by using the vortex technique. Then, the glucose biosensing assay (mentioned below) was added to the polymer blend.

GOX (5 µL of 0.4 mg mL^{-1}) (AG Scientific, Spain) solution, a 5 µL of 0.05 mg mL^{-1} HRP (Sigma–Aldrich, Spain) solution and a 5 µL TMB (Sigma–Aldrich, Spain) in dimethyl sulfoxide (DMSO) (>99.7%, Sigma–Aldrich, Spain) (TMB:DMSO, 24:2.25) solution were mixed with 30 µL of the TNT/C_8-Fe/alginate polymer suspension. The suspension was vortexed for 10 s. A $CaCl_2$ bath was prepared by filling, with a 2 mL (10 mm height) of 0.2 M $CaCl_2$ (93%, Sigma–Aldrich, Spain) solution in a 5 mL glass beaker. A vertical gradient magnetic field was supplied to the bath by keeping a NdFeB permanent magnet (cubic 10 mm magnet, surface 495 mT) right under the beaker. Then, 20 µL of the assay polymer mixture was dripped into the $CaCl_2$ bath to form the Janus bead. The volume of the dripping drop determines the dimensions of the bead. This dimension can be modulated by using other volumes of the solution. Instantly, the polymer droplet was attracted to the depth of the beaker while cross-linking with the calcium ions, under the magnetic field. The magnetic particles stay at the bottom of the bead since they get trapped due to the polymerization process. The Janus bead was kept in the bath for 3 min. Then, the scaffold was washed with distilled water for 30 s. The obtained scaffolds were air dried for 2 min. to evaporate extra surface water and used at the same time.

Colorimetric Signal Readout Analysis: The Janus beads were kept inside 1 mL of whole blood diluted with water and PBS (10 and 100 times) to test the performance of the beads in the presence of RBCs. After 6 min, the beads were removed from the baths and rinsed with water/PBS. Then, the colorimetric signal (top of the bead – Figure 1b) was captured by a Sony Cyber-shot DSC-RX100 camera, over time, under controlled light conditions. For the paper scaffold, circles of 0.7 cm diameter were printed on cellulose filter paper, Whatman filter paper #1 (Sigma Aldrich, Spain) by a Xerox ColorQube 8570 wax printer and the wax barriers were generated with a FLC oven, set at 125 °C for 5 min. Next, a 20 µL of the enzymatic and colorimetric assay [same ratios as in the Experimental Section (Fabrication of the Janus Bead) without TNT/ C8-Fe/alginate nanocomposite] was drop-casted onto the sensing region of the paper and allowed to absorb in the paper for 10 min. Then, 15 µL of blood was added to the sensing area and the paper was slightly rinsed with PBS solution after 6 min. Finally, the sensing area image was captured.

Glucose Determination by the Janus Bead: Three glucose calibration systems were prepared by using phosphate-buffered saline (PBS) (137 mM NaCl, 2.7 mM KCl and 10 mM phosphate buffer solution, pH 7.4 at 25 °C, Sigma–Aldrich, Spain), human serum (H4522, from human male AB plasma, USA origin, Sigma–Aldrich, USA) and whole blood solution (use approved by the "comité de ética para las investigaciones con seres humanos, sus muestras y sus datos" (CEISH-UPV/EHU), code:TI0175). For the PBS calibration, first 10 mM glucose solution (in PBS) was prepared and then, it was diluted with PBS to obtain the desired glucose concentrations. Whole blood and plasma were used to make the calibration curves within the range of 0.1–0.8 mM. The plasma, with a 5 mM preexistent glucose level (measured using a commercial glucometer (Freestyle Freedom Lite Abbott glucose meter, UK)), was diluted with PBS to obtain the desired glucose values (0.1–0.8 mM). However, the glucose meter was not able to read the preexistent glucose level in the whole blood, due to the low blood glucose levels (<1 mM) of the sample. Therefore, externally spiked glucose (10 mM glucose stock blood solution) was prepared and later diluted with PBS to obtain the 0.1–0.8 mM glucose levels for the calibration curve.

To check the glucose levels through the Janus beads, 15 µL of the glucose samples were pipetted over the Janus beads, placed on a glass slide, and the images of the beads were captured at 0 and 6 min by a Sony Cybershot DSC-RX100 camera, over time, under controlled light conditions. Finally, the obtained images were analyzed by Image J software.[34]

In the case of blood analysis, the beads were rinsed with water to remove surface adhered blood layer. Then, the images were taken and analyzed by Image J software.[34] In all cases, the intensities of the images were analyzed by mean grey value (black and white, B&W value) 0–255 scale (black = 0, white = 255). The difference between the B&W values at 0 and at 6 min was related to the corresponding glucose concentration.

Characterization: Scanning electron microscopy (SEM) images of the freeze-dried beads were recorded by a Field Emission Scanning Electron Microscope S-4800 (Hitachi Japan) and a Carl Zeiss EVO 40 (Oberkochen, Germany) equipped with an EDS Oxford Instrument X-Max detector (Abingdon, UK). Magnetization measurements for the iron oxide nanoparticles and the dehydrated beads were carried out in a 7 T Quantum Design MPMS3 SQUID (Superconducting Quantum Interference Device) and homemade VSM (vibrating-sample magnetometer) magnetometer at room temperature. Data, statistical, and image analysis were carried out in Excel, Origin Pro 2018, and Image-J.

Supporting Information

Supporting Information is available from the Wiley Online Library or from the author.

Acknowledgements

The authors acknowledge the MaMi project, funded by the European Union's Horizon 2020 research and Innovation Programme under grant agreement no. 766007. The authors acknowledge funding support from the "Ministerio de Ciencia y Educación de España" under grant PID2020-120313GB-I00/AIE/10.13039/501100011033 y por FEDER una manera de hacer Europa, Gobierno Vasco Dpto. Educación for the consolidation of the research groups (IT1633-22) and Proyecto de Investigación Fundamental Colaborativa – Investigación Fundamental ELKARTEK: KK-2023/00070. Special thanks to (SGIker) of the University of the Basque Country (UPV/EHU) and Dr. Rafael Morales for SQUID characterization.

Conflict of Interest

The authors declare no conflict of interest.

Author Contributions

U.B.G. performed conceptualization, methodology, investigation, wrote the original draft, and reviewed and edited the final manuscript. A.C.-A.,

S.G.-R., and J.M.-R. performed investigation. L.B.-D. performed conceptualization, supervision, acquired resources and funding, and wrote, reviewed, and edited the final manuscript. F.B.-L. performed conceptualization, methodology, supervision, acquired resources and funding, and wrote, reviewed, and edited the final manuscript.

Data Availability Statement

The data that support the findings of this study are available from the corresponding author upon reasonable request.

Keywords

blood, colorimetric glucose, Janus beads, Lab-in-a-Bead, magnetic hydrogels, sensor scaffolds

Received: December 12, 2022
Revised: July 11, 2023
Published online: September 13, 2023

[1] N. A. Rakow, K. S. A. Suslick, *Nature* **2000**, *406*, 710.
[2] X. Han, Y. Liu, Y. Yin, *Nano Lett.* **2014**, *14*, 2466.
[3] A. J. Bandodkar, P. Gutruf, J. Choi, K. H. Lee, Y. Sekine, J. T. Reeder, W. J. Jeang, A. J. Aranyosi, S. P. Lee, J. B. Model, R. Ghaffari, C. J. Su, J. P. Leshock, T. Ray, A. Verrillo, K. Thomas, V. Krishnamurthi, S. Han, J. Kim, S. Krishnan, T. Hang, J. A. B.-F. Rogers, *Sci. Adv.* **2019**, *5*, eaav3294.
[4] U. B. Gunatilake, S. Garcia-Rey, E. Ojeda, L. Basabe-Desmonts, F. Benito-Lopez, *ACS Appl. Mater. Interfaces* **2021**, *13*, 37734.
[5] Z. Wang, Y. Liu, Z. Wang, X. Huang, W. Huang, Z. C. Wang, *View* **2021**, *2*, 20200165.
[6] H. Zhang, E. Smith, W. Zhang, A. Zhou, *Biomed. Microdevices* **2019**, *21*, 48.
[7] S. Garcia-Rey, E. Ojeda, U. B. Gunatilake, L. Basabe-Desmonts, F. Benito-Lopez, *Biosensors* **2021**, *11*, 379.
[8] S. Rafieian, H. Mirzadeh, H. Mahdavi, M. E. Masoumi, *IEEE J. Sel. Top. Quantum Electron.* **2019**, *26*, 154.
[9] N. S. Satarkar, D. Biswal, J. Z. Hilt, *Soft Matter* **2010**, *6*, 2364.
[10] H. Banerjee, M. Suhail, H. Ren, *Biomimetics* **2018**, *3*, 15.
[11] Y. Zhao, Z. Xu, H. Niu, X. Wang, T. Lin, *Adv. Funct. Mater.* **2015**, *25*, 437.
[12] U. B. Gunatilake, M. Venkatesan, L. Basabe-Desmonts, F. Benito-Lopez, *J. Colloid Interface Sci.* **2022**, *610*, 741.
[13] S. Kim, A. U. Regitsky, J. Song, J. Ilavsky, G. H. McKinley, N. I. Holten-Andersen, *Nat. Commun.* **2021**, *12*, 667.
[14] L. Boselli, T. Pomili, P. Donati, P. P. Pompa, *Materials* **2021**, *14*, 1978.
[15] M. Kersaudy-Kerhoas, E. Sollier, *Lab Chip* **2013**, *13*, 3323.
[16] C. Park, H. R. Kim, S. K. Kim, I. K. Jeong, J. C. Pyun, S. Park, *ACS Appl. Mater. Interfaces* **2019**, *11*, 36428.
[17] H. Li, A. J. Steckl, *Anal. Chem.* **2019**, *91*, 352.
[18] C. Park, H. R. Kim, S. K. Kim, I. K. Jeong, J. C. Pyun, S. Park, *ACS Appl. Mater. Interfaces* **2019**, *11*, 36428.
[19] J. Xu, H. Khan, L. Yang, *Anal. Chem.* **2021**, *93*, 14755.
[20] J. Dai, H. Zhang, C. Huang, Z. Chen, A. Han, *Anal. Chem.* **2020**, *92*, 16122.
[21] S. M. Russell, A. Alba-Patiño, M. Borges, R. de La Rica, *Biosens. Bioelectron.* **2019**, *140*, 111346.
[22] S. N. Yin, C. F. Wang, Z. Y. Yu, J. Wang, S. S. Liu, S. Chen, *Adv. Mater.* **2011**, *23*, 2915.
[23] D. H. Kang, H. S. Jung, N. Ahn, S. M. Yang, S. Seo, K. Y. Suh, P. S. Chang, N. L. Jeon, J. Kim, K. Kim, *ACS Appl. Mater. Interfaces* **2014**, *6*, 10631.
[24] I. Braccini, S. Pérez, *Biomacromolecules* **2001**, *2*, 1089.
[25] J. Y. Leong, W. H. Lam, K. W. Ho, W. P. Voo, M. F. X. Lee, H. P. Lim, S. L. Lim, B. T. Tey, D. Poncelet, E. S. Chan, *Particuology* **2016**, *24*, 44.
[26] U. B. Gunatilake, R. Morales, L. Basabe-Desmonts, F Benito-Lopez, *Langmuir* **2022**, *38*, 3360.
[27] U. B. Gunatilake, Y. Alvarez-Braña, E. Ojeda, L. Basabe-Desmonts, F. Benito-Lopez, *J. Mater. Chem. A* **2022**, *10*, 12832.
[28] A. Kauppila, A. Karmenyan, M. Kinnunen, R. Myllylä, *Biomed. Opt. Express* **2011**, *2*, 1803.
[29] G. Turco, I. Donati, M. Grassi, G. Marchioli, R. Lapasin, S. Paoletti, *Biomacromolecules* **2011**, *12*, 1272.
[30] H. P. Erickson, *Biol. Proced. Online* **2009**, *11*, 32.
[31] P. Zhang, D. Sun, A. Cho, S. Weon, S. Lee, J. Lee, J. W. Han, D. P. Kim, W. Choi, *Nat. Commun.* **2019**, *10*, 940.
[32] S. Mahshid, M. Askari, M. S. Ghamsari, *J. Mater. Process. Technol.* **2007**, *189*, 296.
[33] N. Liu, X. Chen, J. Zhang, J. W. Schwank, *Catal. Today* **2014**, *225*, 34.
[34] C. A. Schneider, W. S. Rasband, K. W. Eliceiri, *Nat. Methods* **2012**, *9*, 671.